J. Min. Metall. Sect. B-Metall. 60 (3) (2024) 451 - 460

Journal of Mining and Metallurgy, Section B: Metallurgy

INFLUENCE OF TOOL STEEL ALLOYING ELEMENTS Mo AND Ni ON THE FORMATION OF THE INTERACTION LAYER BETWEEN TOOL STEELS AND MOLTEN ALUMINIUM ALLOYS

M. Vončina*, T. Balaško, J. Medved, A. Nagode

University of Ljubljana, Faculty of Natural Sciences and Engineering, Department for Materials and Metallurgy, Ljubljana, Slovenia

(Received 03 July 2024; Accepted 25 December 2024)

Abstract

The alloying elements present in both tool steel and aluminium are influenced in the dissolution of tool steels in molten aluminum alloys. This study aims to predict how the alloying elements in the tool steel, particularly nickel (Ni) and molybdenum (Mo), impact the formation of the interaction layer between the tool steel and the molten aluminium alloy. The interaction layer between the investigated tool steels Dievar or RavnexHD and the aluminium alloys Al99.9 and Al99.7 consists of an intermetallic and a composite layer. The interaction layer between the investigated tool steels and the AlSi12 aluminium alloy consists of three different interaction layers. The hot-work tool steel RavnexHD shows the better solubility resistance in various molten aluminium alloys. The main alloying element in the tool steels investigated that has an influence on the dissolution of tool steel in molten aluminium is Ni, which is present in higher amounts in RavnexHD. Ni incorporate in the matrix, and inhibits the diffusion of iron and aluminium through the matrix. Mo in Dievar tool steel forms carbides, allowing easier diffusion of these elements through the Fe-matrix. The resilience in molten aluminium alloys is demonstrated by Ravnex HD tool steel for hot work.

Keywords: *Tool steel–molten aluminum interaction; Interaction layers; Intermetallic phases; Dissolution; Thermodynamics*

1. Introduction

According to the AISI classification of tool steels, Dievar and RavnexHD steels belong to the H group (hot-work tool steels). These steels are generally used at elevated temperatures and fall into three main groups: chromium, tungsten, and molybdenum steels. These steels have excellent resistance to softening at high temperatures, even when exposed to prolonged or cyclic temperature stresses [1–6]. Nickel is added to the steel to stabilize the austenitic structure, which increases its toughness, ductility, and corrosion resistance at low temperatures. In some cases, nickel can also increase the strength of steel. Nickel can improve the machinability of steel, making it easier to process using methods such as cutting, drilling, and turning. Molybdenum increases the strength and hardness of steel, especially at elevated temperatures. Molybdenum improves the wear resistance of steel, which is important for applications where components are subjected to friction and abrasion. Molybdenum improves the creep strength of steel, meaning it retains its strength even at high temperatures [4, 5]. The tool steels investigated were originally developed for the manufacture of die-casting tools made of aluminium alloys and belong to the group of chromium hot-work tool steels. During the thoughtful development, the needs of the market, as well as the end users of the tools, were taken into account [1, 7]: the steel can be hardened in the air from a relatively low austenitization temperature, small dimensional changes during hardening, good oxidation resistance during cooling in air, resistance to erosion due to contact with aluminium melt and thermal fatigue, as well as an optimal content of alloying elements and an acceptable price. Several authors [8–12] have investigated the effects of elevated temperatures on the mechanical and physical properties of hot-work tool steels.

The main characteristics of this group of tool steels are high toughness and resistance to temperature shocks. Steels work well in a wide temperature range, mainly due to the low content of carbon and alloying elements. At the same time, they also have good hardenability and should be cooled in the furnace after forging. During heat treatment, it is

Corresponding author: maja.voncina@ntf.uni-lj.si

https://doi.org/10.2298/JMMB240703036V

recommended that chromium hot-work tool steels should be in a protective atmosphere, mainly due to carburization and decarburization. To reduce hardening distortion, it is recommended to anneal the steels to eliminate stress before final processing and heat treatment [1, 3–5, 13]. Molybdenum is usually added to chromium hot-work tool steels, which together with chromium inhibits the diffusion-dependent transformations of austenite [14, 15]. The zones where the pearlitic and bainite transformations begin are separate. However, due to the low carbon content, the hardness of the phases formed during the pearlite transformation is low, and at the same time, the martensite start temperature (MS) is relatively high. If the cooling rates are high enough, the hardened microstructure consists mainly of martensite and some residual austenite. Despite the medium carbon content, a pre-eutectoid phase is formed in chromium hot-work tool steels, namely vanadium MC carbide, which may also contain molybdenum and chromium, and small contents of silicon and iron [1, 6].

The interaction layer between the tool steel and the aluminium alloy consists of an intermetallic layer along with a composite layer [16]. The thickness of this interface layer is affected by the presence of alloying elements in both the molten aluminium and the tool steel. Alloying elements found in the tool steel, including chromium, manganese, silicon, molybdenum, and vanadium, participate in the formation of carbides such as Cr-based ($M_{23}C_6$) and V-based (MC) within the interface layer [15]. These elements play a role in minimizing or preventing the formation of an intermetallic layer, with silicon exerting the most significant influence [17]. Ni also reduces the activity of aluminium in the ferrite matrix and causes a reduction in the thickness of the intermetallic layer [15]. Moreover, the iron content within the aluminium alloy impacts the thickness of the lower layer; however, excessively high iron content is discouraged due to the formation of detrimental acicular phases that compromise mechanical properties. Additionally, the temperature of the aluminium melt also plays a crucial role, as higher temperatures result in a thicker interface layer [15, 18–20]. Moreover, protective coatings on tool surfaces can improve corrosion resistance, thermal fatigue and wear resistance [21–25].

This study aims to predict how the alloying elements in tool steel, particularly nickel (Ni) and molybdenum (Mo), impact the formation of the interaction layer between the tool steel and the molten aluminium alloy. To examine the impact of tool steel alloying elements on the interaction layer formed between the studied tool steel and various aluminium alloys, a DSC analysis was conducted at 700 °C for 12 h. The findings were further validated and supported through comprehensive SEM and EDS analysis.

2. Experimental

To examine the interaction layer formed between the studied aluminium alloys Al99.9, Al99.7 and AlSi12 and the tool steels Dievar and RavnexHD (chemical compositions are presented in Table 1) in the quenched and tempered condition, isothermal DSC measurements were performed at a temperature of 700 °C for 12 h. The measurements were conducted using a NETZSCH STA Jupiter 449C instrument in an argon atmosphere. The temperature was increased to 700 °C at a rate of 20 K min^{-1}, held for 12 h, and then cooled to room temperature at the same rate. The tool steel specimens were 4 mm in diameter and 1 mm in height, while the aluminium alloy samples measured 4 mm in diameter and 3 mm in height. All sample surfaces were polished with Struers Abramin Metal Polisher using grinding paper of 1200 to ensure good contact. The samples were arranged in a corundum crucible, with the tool steel placed at the bottom and the aluminium alloy on top.

After the DSC measurements, the samples were prepared for metallographic analysis. The samples were ground using the Struers Abramin Metal Polisher with abrasive papers of grit sizes: 180, 240, 400, 800, 1200, and 2000, whereas wet grinding with water was used. This was followed by polishing with diamond paste. The thickness of the interaction layer in all samples was examined using an Olympus BX61 light microscope. The composition of the interaction layers and the chemical composition of the Fe-bearing phases were analyzed to identify the types of phases formed. This analysis was performed with a Thermo Fisher Scientific Quattro S FEG SEM microscope, equipped with an Oxford Ultim® Max EDS analyzer.

Thermodynamic calculations were performed using Thermo-Calc software to analyze the microstructural components of the investigated steels. The TCFE12 database and Thermo-Calc version 2024a were utilized for this purpose. The software also assessed the thermodynamic stability of carbides

Table 1. *The chemical composition (% by weight) of the tool steels analyzed*

Element	C	Si	Cr	Ni	V	Mn	Mo	Nb	N	Fe
Dievar	0.34	0.17	5.05	0.19	0.54	0.44	2.37	0.002	0.006	Rest
RavnexHD	0.36	0.3	5	1.65	0.6	0.4	1.7	0.003	0.02	Rest

after tempering at 700 °C and simulated the effect of alloying elements on aluminium activity within the ferritic matrix.

3. Results and discussion

3.1. DSC analysis

According to Fig. 1, the DSC analysis shows a faster dissolution of Dievar tool steel compared to RavnexHD in molten pure aluminium (Al99.9). This is indicated by the sharper decrease in the DSC curve for Dievar. When exposed to aluminium alloys Al99.7 or AlSi12, the decrease in the DSC curves is even faster for both steels. This suggests a thicker layer forming between the tool steel and the aluminium alloy, and a more rapid dissolving of the steel. The difference in the interaction layer thickness is expected to be larger between Dievar and RavnexHD when exposed to Al99.7, based on the already observed bigger difference for pure aluminium. The dissolution process is faster initially because the interaction layer is thin, presenting a shorter diffusion path for the dissolving elements. Over time, this process slows down as the interaction layer thickens, making diffusion more difficult.

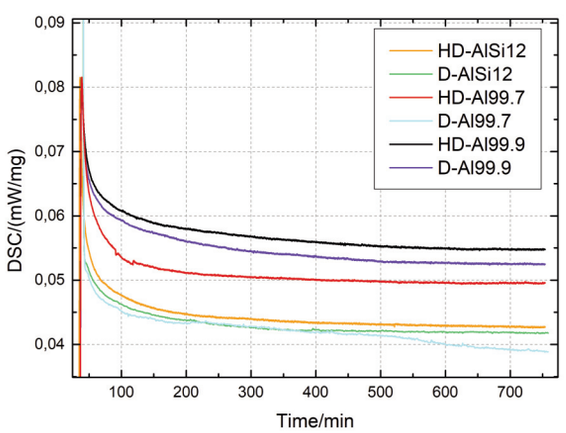

Figure 1. *DSC curves showing the dissolution of Dievar and RavnexHD tool steels in Al99.9, Al99.7, and AlSi12 aluminium alloys at 700 °C.*

3.2. Thicknesses of the interaction layers

Fig. 2 shows microscopic images of all tested samples. As reported in previous research [16, 18, 19], the interaction layers for both tool steels in contact with Al99.9 and Al99.7 alloys consist of two layers: an interaction layer and a composite layer. The interaction layer with the Al99.7 alloy is slightly thinner compared to Al99.9, likely due to the presence of alloying elements. This aligns with findings from other studies [16, 18, 19, 26–28]. For example, adding iron to the molten aluminium can reduce the intermetallic layer thickness. This happens because once the iron content reaches saturation, the driving force for iron diffusion (chemical potential gradient) from the tool steel to the melt weakens significantly [29]. Higher iron content in the melt also promotes the formation of Fe-containing intermetallic compounds within the cast structure. Therefore, it's recommended to keep the iron content in aluminium die-casting alloys at or below 1.1 wt.% [30]. When exposed to the AlSi12 alloy, the interaction layer for both tool steels is more complex, consisting of three distinct layers. The total thickness of the interaction layer for Dievar is around 490 µm, with a composite layer of about 550 µm. For RavnexHD, these values are approximately 320 µm and 330 µm, respectively. These layer thickness measurements from the micrographs support the initial assumptions based on the DSC curves.

3.3. Thermodynamic simulations – carbide formation

Prior to further metallographic analysis, the results of the thermodynamic calculations are shown in Table 2. The table indicates the type of carbides present in each steel analyzed and which carbides remain stable at the chosen analysis temperature of 700 °C. The A_{e1} temperatures for both steels are also given. Notably, the A_{e1} temperature for the RavnexHD steel is 76 °C lower than that of the Dievar steel and is close to the investigated temperature of 700 °C. This indicates that the microstructure of the RavnexHD steel, which currently consists of martensite and carbides as a result of quenching and tempering, could soften faster than the Dievar steel, as 700 °C is already in the region of spheroidal annealing. However, as the RavnexHD steel has a higher Ni content, this could prevent softening.

Since the durability of various tool steels in molten Al99.9, Al99.7, and AlSi12 was investigated at 700 °C, the thermodynamic calculations are presented only for the temperature range of 600 °C to 800 °C (Fig. 3). In Dievar steel (Fig. 3a), three carbide/carbonitride types are stable at 700 °C: $M_{23}C_6$ carbides $(Cr,Fe,Mo)_{23}C_6$, MCN carbonitrides VCN, and M_2C carbides $(Mo,V,Cr)_2C$. The mass fraction of $(Cr,Fe,Mo)_{23}C_6$ is the highest (0.048) of all carbides present in Dievar steel, followed by $(Mo,V,Cr)_2C$ carbides with a mass fraction of 0.010. VCN has the lowest fraction with 0.002 (Table 3). In contrast, only two carbide types are stable in RavnexHD steel (Fig. 3b) at 700 °C: $M_{23}C_6$ $(Cr,Fe,Mo)_{23}C_6$ carbides and MCN carbonitrides VCN. The $(Cr,Fe,Mo)_{23}C_6$

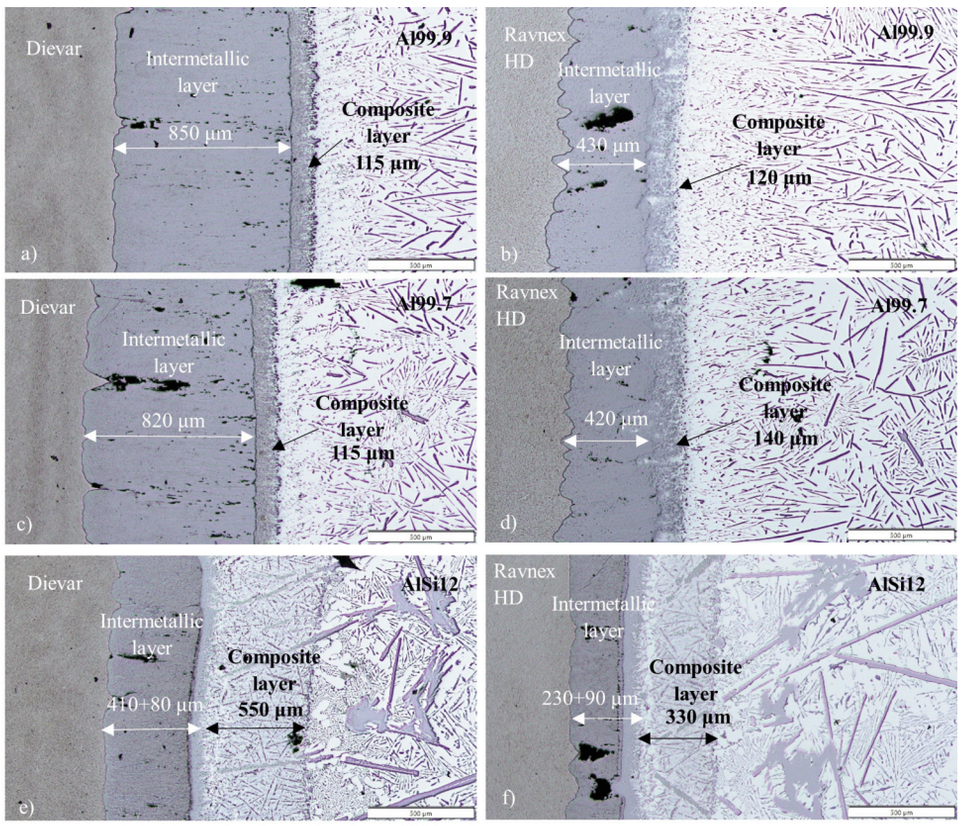

Figure 2. *Micrographs of the interaction layer between Dievar (a, c, e) and RavnexHD (b, d, f) tool steel and Al99.9 (a, b), Al99.7 (c, d) and AlSi12 (e, f) aluminium alloy at 700 °C*

carbides have the highest mass fraction of 0.055, followed by VCN with a mass fraction of 0.006 (Table 3). If the carbide types are compared, the Dievar steel at 700 °C has M_2C carbides, while both steels contain $M_{23}C_6$ carbides and MCN carbonitrides. There are differences in the amount of the individual carbides. steel is expected to have a more stable and resistant microstructure. This means the layers formed should be thinner than those in Dievar steel. One of the main reasons for this is the higher Ni content in RavnexHD steel (1.46 wt.%). Ni is known to be a non-carbide former and has a high solubility in ferrite and

Table 2. *A_{e1} temperature and type of carbides and their precipitation temperature in the analysed steels*

Type of steel	A_{e1} temperature /°C	Type of carbide/carbonitride and its precipitation temperature /°C				
		MCN	M_2C	M_7C_3	$M_{23}C_6$	M_6C
Dievar	808	1099	1012	869	861	636
RavnexHD	732	1219	950	933	846	575

The Dievar steel has a lower mass fraction of $(Cr,Fe,Mo)_{23}C_6$ carbides (difference of 0.007) and a lower fraction of VCN carbonitrides (difference of 0.004). Due to the chemical composition, RavnexHD

Table 3. *Fraction of a phase in analysed steels at 700 °C*

Type of steel	Fraction of a phase in steel at 700 °C			
	Ferrite	$M_{23}C_6$	M_2C	VCN
Dievar	0.94	0.048	0.01	0.002
RavnexHD	0.939	0.055	/	0.006

austenite, which promotes stability. The mass fraction of Ni in the matrix at 700 °C is 0.01731 for RavnexHD and 0.00199 for Dievar, which means that in the case of RavnexHD the Ni fraction in the matrix at 700 °C is 8.7 times higher. The amount of Mo could also play a role in the resistance, as the Dievar steel has a higher content (0.67 wt.%). However, the calculations show that $(Mo,V,Cr)_2C$ carbides are present in the matrix of the Dievar steel and that the Mo content in the matrix at 700 °C is almost the same for both steels (0.00877 for Dievar and 0.00714 for

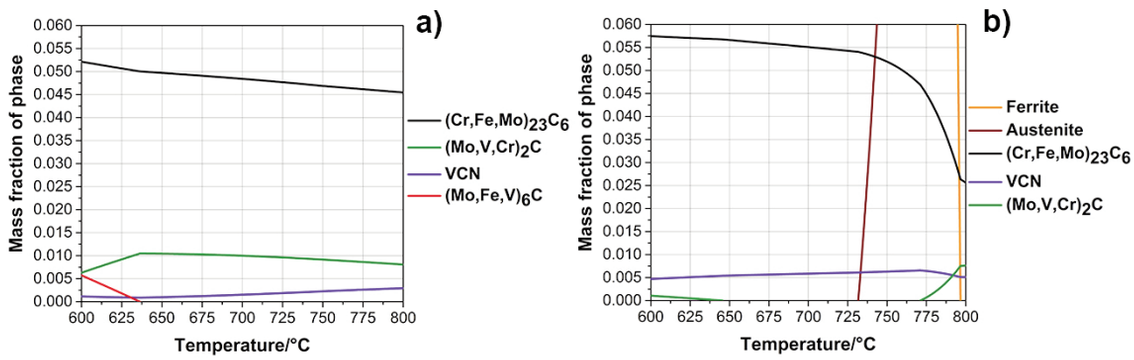

Figure 3. *Thermodynamically calculated diagrams (fraction of all phases as a function of temperature) in the temperature range from 600 °C to 800 °C for Dievar (a) and RavnexHD (b) tool steels*

RavnexHD in mass fraction). This suggests that Ni may be the only important alloying element affecting the resistance of the steel to dissolution in Al alloys. Therefore, the RavnexHD steel can be expected to be more stable at higher temperatures, in this case, 700 °C, than the Dievar steel, although a lower Ae1 temperature was calculated for RavnexHD.

3.4. SEM/EDS analysis

To verify where the alloying elements, especially Ni and Mo, incorporate or which phases they form, the EDS line scans are presented in Fig. 4. All EDS line scans confirm the types of interaction layers as reported in our previous research [15, 18, 19]. One intermetallic layer (Al_5Fe_2) and composite layer (Al_3Fe) formed in the interaction layer in the case of Al99.9 or Al99.7 aluminium alloy in contact with both tool steels investigated. Joining the investigated tool steels with AlSi12 aluminium alloy resulted in forming three distinct layers at the interface. These layers consisted of $Al_5Fe_2(Si)$, $Al_{23}Fe_{17}Si$, and Al_5Fe_2Si (or $Al_8Fe_2Si(Mn)$) with decreasing iron content and increasing aluminium content as you move away from the steel. On the aluminium alloy side, a composite layer formed.

Because the dissolution of Dievar tool steel, which contains a higher concentration of Mo and a lower concentration of Ni, was faster, EDS maps were made to see the type and density of formed carbides in the interaction layers, influencing the dissolution. The density of Mo-based carbides, presumably Mo_6C-type, is much higher in the interaction layer between Dievar tool steel and Al99.7 aluminium alloy. In both cases, V-based carbides, presumably of the VC-type, are also present [31]. In the interaction layer between RavnexHD tool steel and Al99.7 aluminium alloy the tiny layer with higher Ni content, which inhibits the dissolution, can be observed, whereas Ni is also dissolved in Fe-matrix. Regarding these results, dissolved Ni has a much bigger influence on forming the interaction layers between the tool steel and the molten aluminium alloy than Mo in the form of carbides.

3.5. Thermodynamic simulations - activity of the alloying elements

Table 4 and Fig. 6 illustrate the activity of the alloying elements in the ferrite at 700 °C for both steels. Cr and Mo have almost identical activity values in both steels (Table 4); the thickness of the interaction layers is not influenced by them, while the Dievar steel shows slightly higher Al activity in the matrix at 700 °C (Fig. 6b). The key factor for the superior dissolution resistance of the RavnexHD steel remains its Ni content. Table 4 shows a significantly higher Ni activity in RavnexHD compared to Dievar steel at 700 °C. Thus, the Ni activity of RavnexHD is 8.2 times higher at 0 wt.% Al, with this trend continuing at 1 wt.% Al (8.3 times higher) and 10 wt.% Al (8.5 times higher). This is consistent with the mass fraction of Ni dissolved in the matrix for each steel as previously described. Fig. 6c visually confirms this trend and illustrates the significantly higher Ni activity in RavnexHD steel. As already mentioned, Ni stabilizes the matrix, inhibits the diffusion of iron and aluminium through the matrix and inhibits the dissolution of steel in Al alloys.

4. Conclusions

The resilience of two different tool steels Dievar and RavnexHD in molten Al99.9, Al99.7 and AlSi12 aluminium alloy was investigated, and the following conclusions were drawn:

The interaction layer between the investigated tool steels and the Al99.9 and Al99.7 aluminium alloy consists of an intermetallic and a composite layer. The interaction layer between the investigated tool steels

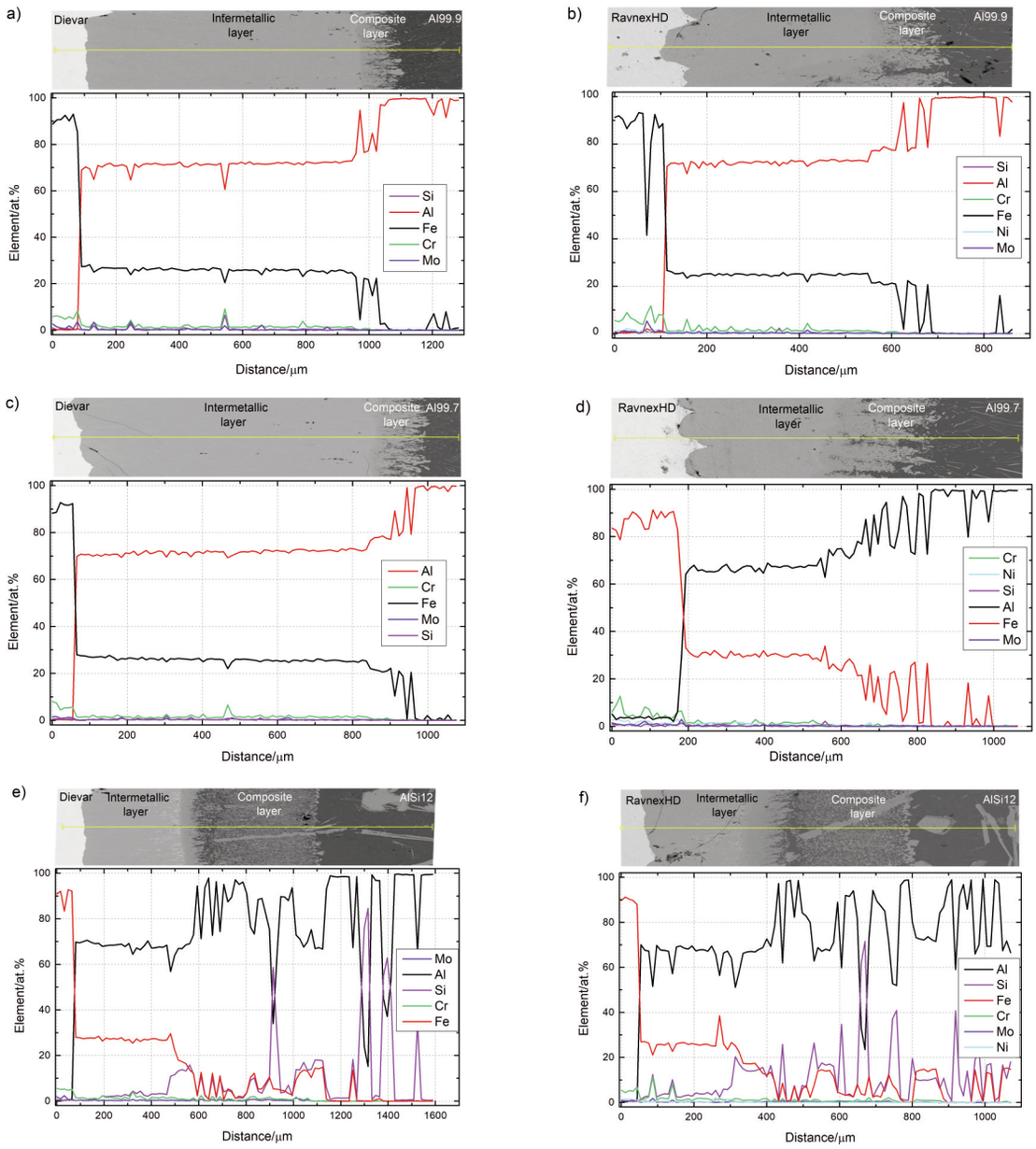

Figure 4. *EDS line-scan of the interaction layers of the Dievar (a, c, e) and RavnexHD (b, d, f) tool steel samples tested at 700 °C in Al99.9 (a, b), Al99.7 (c, d) and AlSi12 (e, f) molten aluminium alloys. The corresponding EDS results are presented in at.%*

Table 4. *The activity of alloying elements in investigated tool steels with different aluminium contents (0, 1 and 10 wt.%)*

Steel type	Activity of a component in ferrite at 700 °C						
	Al	Si	Cr	Ni	V	Mn	Mo
Dievar / 0 wt.% Al	/	$1.66 \cdot 10^{-10}$	0.125	$1.5 \cdot 10^{-3}$	$2.3 \cdot 10^{-4}$	$8.0 \cdot 10^{-3}$	$9.1 \cdot 10^{-2}$
Dievar / 1 wt.% Al	$3.2 \cdot 10^{-7}$	$2.95 \cdot 10^{-10}$	0.126	$1.3 \cdot 10^{-3}$	$2.4 \cdot 10^{-4}$	$8.7 \cdot 10^{-3}$	$8.0 \cdot 10^{-2}$
Dievar / 10 wt.% Al	$1.5 \cdot 10^{-4}$	$4.92 \cdot 10^{-9}$	0.087	$0.1 \cdot 10^{-3}$	$5.3 \cdot 10^{-5}$	$5.4 \cdot 10^{-3}$	$4.5 \cdot 10^{-2}$
RavnexHD / 0 wt.% Al	/	$2.22 \cdot 10^{-10}$	0.112	$12.4 \cdot 10^{-3}$	$1.7 \cdot 10^{-4}$	$6.7 \cdot 10^{-3}$	$7.5 \cdot 10^{-2}$
RavnexHD / 1 wt.% Al	$3.0 \cdot 10^{-7}$	$4.01 \cdot 10^{-10}$	0.116	$10.4 \cdot 10^{-3}$	$2.1 \cdot 10^{-4}$	$7.3 \cdot 10^{-3}$	$7.5 \cdot 10^{-2}$
RavnexHD / 10 wt.% Al	$1.2 \cdot 10^{-4}$	$4.94 \cdot 10^{-9}$	0.087	$0.9 \cdot 10^{-3}$	$5.5 \cdot 10^{-5}$	$4.7 \cdot 10^{-3}$	$4.5 \cdot 10^{-2}$

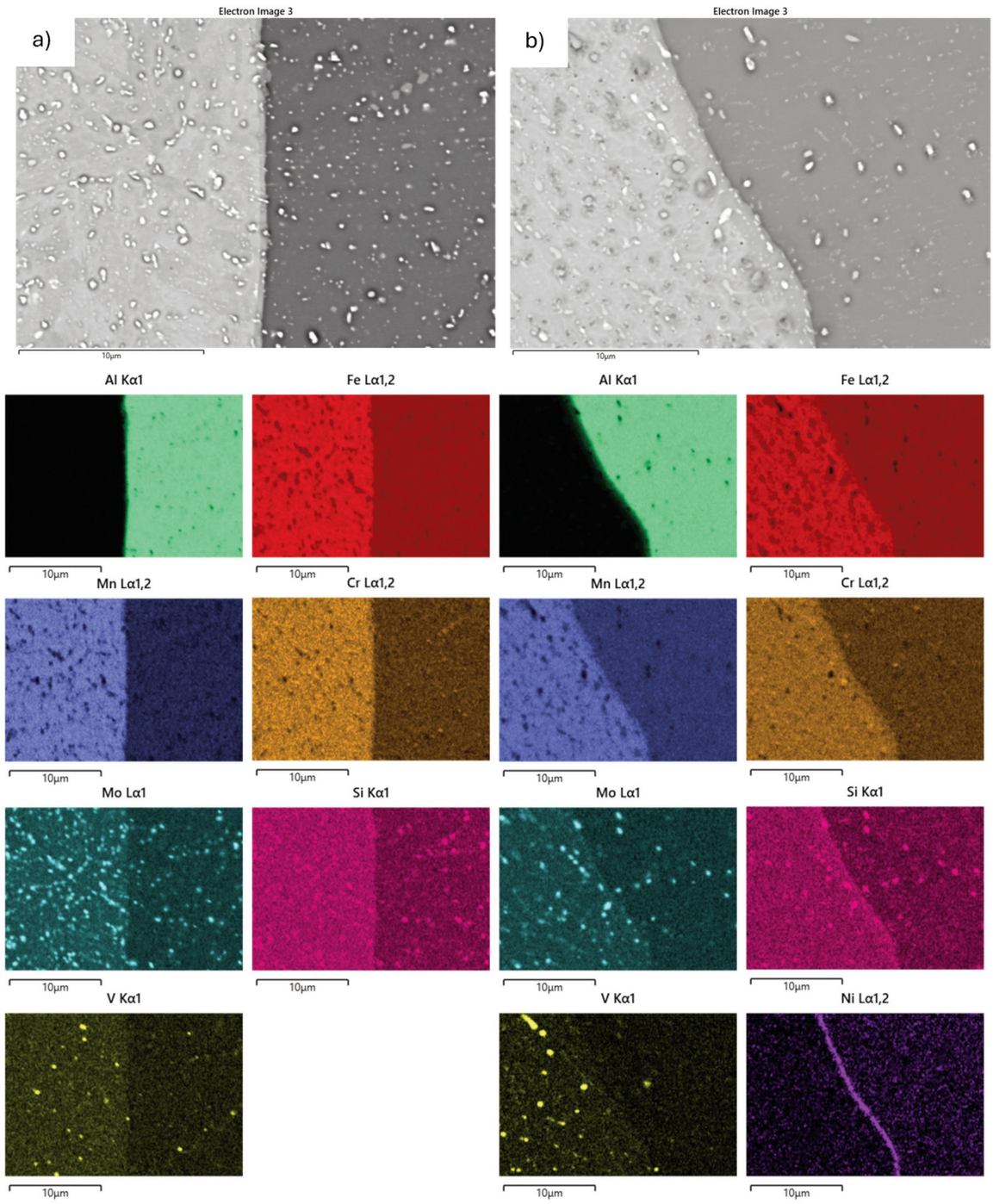

Figure 5. *SEM micrographs of the intermetallic layer in samples Dievar-Al99.7 (a) and RavnexHD-Al99.7 (b) and its corresponding elemental maps (EDS)*

and the AlSi12 aluminium alloy consists of three different interaction layers.

The hot-work tool steel RavnexHD shows the better solubility resistance in various molten aluminium alloys. The main alloying element in the tool steels investigated, that affects the dissolution of tools in molten aluminium is Ni, which is present in higher amounts in RavnexHD.

Ni incorporate in the matrix, inhibits the diffusion of iron and aluminium through the matrix. Mo, on the other hand, forms carbides in Dievar tool steel, allowing easier diffusion of these elements through

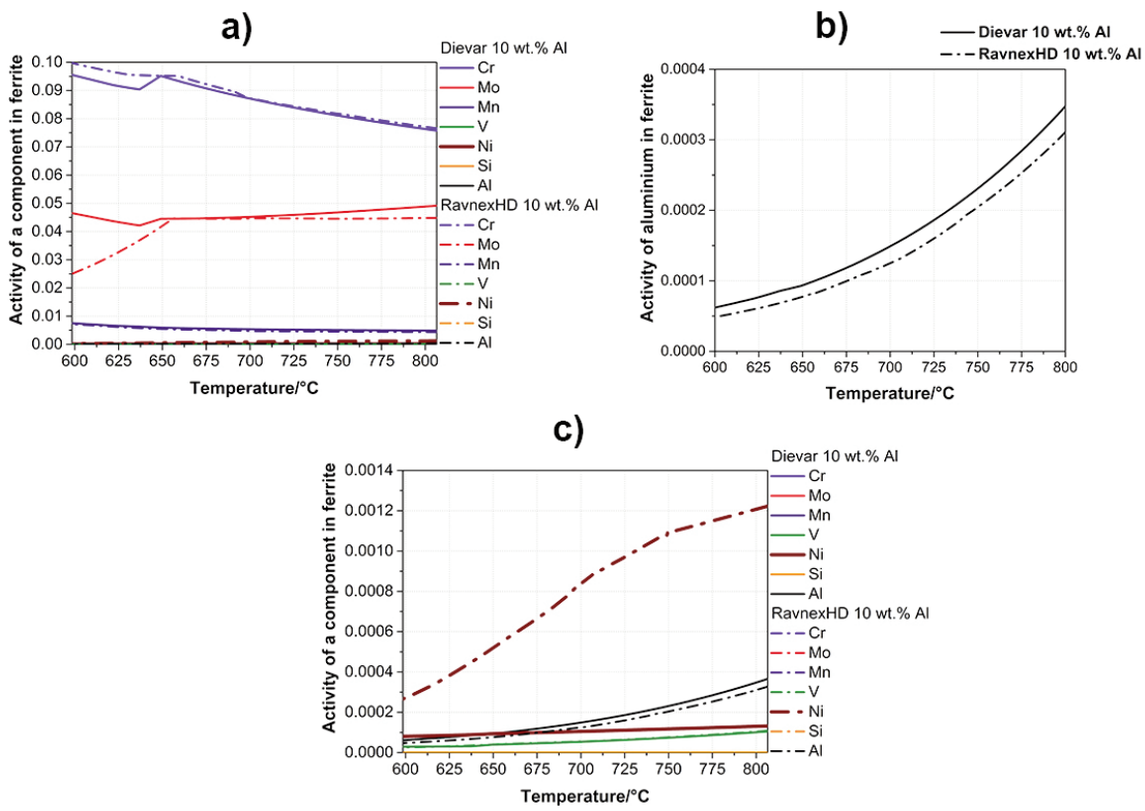

Figure 6. *Effect of Ni and Mo on the activity of a component in ferrite for Dievar and RavnexHD (a) and activity of aluminium in ferrite for Dievar and RavnexHD, considering 10 wt.% Al (b)*

the Fe-matrix.

There are still many other open questions and investigation options to be addressed. One of these is, for instance, the influence of other possible alloying elements in the presence of molybdenum and nickel in the tool steels. The second is the use of other investigation methods, e.g. XRD.

Funding

This research was funded by the Slovenian Research and Innovation Agency (ARIS) under the Advanced Metallurgy program, grant number P2-0344(B).

Author contributions

M.V.: Conceptualization, Methodology, Investigation, Validation, Writing—review & editing; T.B.: Investigation, Validation, Writing—review & editing; J.M.: Writing—review & editing; A.N.: Conceptualization, Investigation, Writing—review & editing. All authors have read and agreed to the published version of the manuscript.

Data Availability Statement

Not applicable. If needed it will me provided by the Authors.

Conflicts of Interest

The authors declare no conflict of interest.

References

[1] G. Roberts, G. Krauss, R. Kennedy, Tool Steels: 5th ed., ASM International, Materials Park, 1998, p. 364.

[2] C. Højerslev, Tool steels, Risø National Laboratory, Roskilde, 2001, p. 25.

[3] C.R. Sohar, Lifetime controlling defects in tool steels, Springer, Berlin, 2011, p. 224.

[4] R.A. Mesquita, Tool steels: properties and performance, CRC Press, Boca Raton, 2016, p. 245.

[5] ASM handbook, volume 1: Properties and selection: irons, steels, and high-performance alloys, ASM International, Materials Park, 1990, p. 1063. https://doi.org/10.31399/asm.hb.v01.9781627081610

[6] H. Essoussi, S. Ettaqi, E.H. Essadiqi, From the alloy design to the microstructural and mechanical properties of medium manganese steels of the third generation of advanced high strength steels, Journal of Mining and Metallurgy, Section B: Metallurgy, 60(3) (2024) 339-

352. https://dx.doi.org/10.2298/jmmb240601028e

[7] G. Krauss, Tool materials for molds and dies: application and performance: proceedings, Golden, CO: Colorado School of Mines, 1987, p. 381.

[8] A. Medvedeva, J. Bergström, S. Gunnarsson, J. Andersson, High-temperature properties and microstructural stability of hot-work tool steels, Materials Science and Engineering A, 523 (2009) 39-46. https://doi.org/10.1016/j.msea.2009.06.010

[9] Z. Zhang, D. Delagnes, G. Bernhart, Microstructure evolution of hot-work tool steels during tempering and definition of a kinetic law based on hardness measurements, Materials Science and Engineering A, 380 (2004) 222–230. https://doi.org/10.1016/j.msea.2004.03.067

[10] N. Mebarki, D. Delagnes, P. Lamesle, F. Delmas, C. Levaillant, Relationship between microstructure and mechanical properties of a 5% Cr tempered martensitic tool steel, Materials Science and Engineering A, 387-389 (2004) 171-175. https://doi.org/10.1016/j.msea.2004.02.073

[11] A. Jilg, T. Seifert, Temperature dependent cyclic mechanical properties of a hot work steel after time and temperature dependent softening, Materials Science and Engineering A, 721 (2018) 96-102. https://doi.org/10.1016/j.msea.2018.02.048

[12] D. Caliskanoglu, I. Siller, R. Ebner, H. Leitner, F. Jeglitsch, W. Waldhauser, Thermal fatigue and softening behavior of hot work tool steels, Proc. 6th International Tooling Conference, 10-13 September, Karlstad, Sweden, 2002, p. 707-719.

[13] Heat treater's guide: practices and procedures for irons and steels. Metals Park, ASM International, 1995, p. 904.

[14] G.E. Totten, Steel heat treatment: metallurgy and technologies, Boca Raton, FL: CRC Press, 2006, p. 848.

[15] C.W. Wegst, Stahlschlüssel: key to steel, Marbach: Verlag Stahlschlüssel Wegst, 1992, p. 612.

[16] M. Vončina, T. Balaško, J. Medved, A. Nagode, Interface reaction between molten Al99.7 aluminum alloy and various tool steels, Materials, 14 (2021) 7708. https://doi.org/10.3390/ma14247708

[17] K.A. Nazari, S.G. Shabestari, Effect of micro alloying elements on the interfacial reactions between molten aluminum alloy and tool steel, Journal of Alloys and Compounds, 478 (2009) 523-530. https://doi.org/10.1016/j.jallcom.2008.11.127

[18] D. Klobčar, J. Tušek, B. Taljat, Thermal fatigue of materials for die-casting tooling, Materials Science and Engineering A, 472 (2008) 198-207. https://doi.org/10.1016/j. msea.2007.03.025

[19] M. Vončina, S. Kores, A. Nagode, J. Medved, Study of interaction between molten aluminium and hot-work tool steel using DSC method, Journal of Thermal Analysis and Calorimetry, 146 (2021) 1091-1099. https://doi.org/10.1007/s10973-020-10069-3

[20] M. Vončina, A. Nagode, J. Medved, T. Balaško, Influence of temperature on the interaction kinetics between molten aluminium alloy Al99.7 and tool steel H11, Materials and Technology, 57 (2023) 99-103. https://doi.org/10.17222/mit.2023.825

[21] M. Vončina, A. Nagode, J. Medved, T. Balaško, Interaction kinetics between molten aluminium alloy Al99.7 and H11 tool steel with and without an AlCrN protective coating, Applied Surface Science Advances, 18 (2023) 1-7. https://doi.org/10.1016/j.apsadv.2023.100474

[22] M. Ortiz-Domínguez, M. Keddam, Á.J. Morales-Robles, Characterizations and boron diffusion modelling on the AISI H13 steel, Journal of Mining and Metallurgy, Section B: Metallurgy, 60(3) (2024), 353-365. https://doi.org/10.2298/JMMB240423029O

[23] M. Benke, Zs. Salyi, G. Kaptay, Investigation of dissolution resistance of blank and gas-nitrided carbon steels in stationary SAC305 solder alloy melt, Journal of Mining and Metallurgy, Section B: Metallurgy, 54 (3) (2018) 283-290. https://doi.org/10.2298/JMMB170918019B

[24] A. Bjerke, F. Lenrick, A. Hrechuk, K. Slipchenko, R. M'Saoubi, J.M. Andersson, V. Bushlya, On chemical interactions between an inclusion engineered stainless steel (316L) and (Ti,Al)N coated tools during turning, Wear, 532-533 (2023) 205093. https://doi.org/10.1016/j.wear.2023.205093

[25] A. Bjerke, F. Lenrick, S. Norgren, H. Larsson, A. Markström, R. M'Saoubi, I. Petrusha, V. Bushlya, Understanding wear and interaction between CVD α-Al_2O_3 coated tools, steel, and non-metallic inclusions in machining, Surface and Coatings Technology, 450 (2022) 128997. https://doi.org/10.1016/j.surfcoat.2022.128997

[26] M. Yan, Z. Fan, Review Durability of materials in molten aluminum alloys, Journal of Materials Science, 36 (2001) 285-295. https://doi.org/10.1023/A:1004843621542

[27] F. Yin, M. Zhao, Y. Liu, Z. Li, Effect of Si on growth kinetics of intermetallic compounds during reaction between solid iron and molten aluminium, Transactions of Nonferrous Metals Society of China, 23 (2013) 556-561. https://doi.org/10.1016/S1003-6326(13)62499-1

[28] S. Hwang, J. Song, Y. Kim, Effects of carbon content of carbon steel on its dissolution into a molten aluminium alloy, Materials Science and Engineering A, 390 (2005) 437-443. https://doi.org/10.1016/j.msea.2004.08.062

[29] G.B. Winkelman, Z.W. Chen, D.H. St. John, M.Z. Jahedi, Morphological features of interfacial intermetallics and interfacial reaction rate in Al–11Si–2.5Cu–(0.15/0.60)Fe cast alloy/die steel couples, Journal of Materials Science, 39 (2004) 519-528. https://doi.org/10.1023/B:JMSC.0000011507.38552.19

[30] K.N. Obiekea, S.Y. Aku, D.S. Yawas, Effect of pressure on the mechanical properties and microstructure of die cast aluminium A380 alloy, Journal of Minerals and Materials Characterization and Engineering, 2 (2014) 248-258. http://dx.doi.org/10.4236/jmmce.2014.23029

[31] G. Xu, K. Wang, X. Dong, H. Jiang, Q. Wang, B. Ye, W. Ding, Multiscale corrosion-resistance mechanisms of novel ferrous alloys in dynamic aluminum melts, Corrosion Science, 163 (2020) 108276. https://doi.org/10.1016/j.corsci.2019.108276

UTICAJ ELEMENATA ZA LEGIRANJE ALATNOG ČELIKA Mo I Ni NA FORMIRANJE SLOJA INTERAKCIJE IZMEĐU ALATNIH ČELIKA I RASTOPLJENIH LEGURA ALUMINIJUMA

M. Vončina, T. Balaško, J. Medved, A. Nagode

Univerzitet u Ljubljani, Prirodno tehnološki fakultet, Katedra za materijale i metalurgiju, Ljubljana, Slovenija

Apstrakt

Legirajući elementi prisutni i u alatnom čeliku i u aluminijumu utiču na rastvaranje alatnih čelika u rastopljenim legurama aluminijuma. Ova studija ima za cilj da predvidi kako legirajući elementi u alatnom čeliku, posebno nikl (Ni) i molibden (Mo), utiču na formiranje sloja interakcije između alatnog čelika i rastopljene legure aluminijuma. Interakcioni sloj između ispitivanih alatnih čelika Dievar ili RavnekHD i legura aluminijuma Al99.9 i Al99.7 sastoji se od intermetalnog i kompozitnog sloja. Interakcioni sloj između ispitivanih alatnih čelika i legure aluminijuma AlSi12 sastoji se od tri različita interakcijska sloja. Alatni čelik za rad u toplom stanju RavnekHD pokazuje bolju otpornost na rastvorljivost u različitim legurama istopljenog aluminijuma. Glavni legirajući element u ispitivanim alatnim čelicima koji utiče na rastvaranje alatnog čelika u rastopljenom aluminijumu je Ni, koji je u većim količinama prisutan u RavnekHD. Ni se ugrađuje u matricu i inhibira difuziju željeza i aluminijuma kroz matricu. Mo u Dievar alatnom čeliku formira karbide, omogućavajući lakšu difuziju ovih elemenata kroz Fe-matricu. Otpornost u rastopljenim aluminijumskim legurama pokazuje čelik za rad u toplom stanju RavnekHD.

Ključne reči: *Interakcija alatnog čelika i rastopljenog aluminijuma; Slojevi interakcije; Intermetalne faze; Rastvaranje; Termodinamika*